Vision Based Mobile Target Geo-localization and Target Discrimination using Bayes Detection Theory

Rajnikant Sharma, Josiah Yoder, Hyukseong Kwon, Daniel Pack

Abstract In this paper, we develop a technique to discriminate ground moving targets when viewed from cameras mounted on different fixed wing unmanned aerial vehicles (UAVs). First, we develop a extended kalman filter (EKF) technique to estimate position and velocity of ground moving targets using images taken from cameras mounted on UAVs. Next, we use Bayesian detection theory to derive a log likelihood ratio test to determine if the estimates of moving targets computed at two different UAVs belong to a same target or to two different targets. We show the efficacy of the log likelihood ratio test using several simulation results.

1 Introduction

Over the past decade, there has been an increase in the use of Unmanned Aerial Vehicles (UAVs) in several military and civil application that are considered dangerous for human pilots. These applications include surveillance [1], reconnaissance [2], search [3], and fire monitoring [4, 5]. Among the suite of possible sensors, a video camera is inexpensive, lightweight, fits the physical requirements of small fixed wing UAVs, and has a high information to weight ratio. One of the important applications of camera equipped fixed wing UAVs is determining the location of a ground target when imaged from the UAV. The target is geo-localized using the pixel location of the target in the image plane, the position and attitude of the air vehicles, the camera's pose angles, and knowledge of the terrain elevation. Previous target localization work using a camera equipped UAV is reported in [6, 7, 8, 9] and references therein. Barber *et al.* [7] used a camera, mounted on a fixed-wing UAV, to geo-localize a stationary target. They discussed recursive least square (RLS) filtering, bias estimation, flight path selection, and wind estimation to reduce the localization

R. Sharma, J. Yoder, H. Kwon, and D. Pack
Academy Center for UAS Research, US Air Force Academy, Colorado, e-mail: (rajnikant.sharma.ctr.in, josiah.yoder.ctr, hyukseong.kwon, daniel.pack)@usafa.edu

errors. Pachter *at el.* [6] developed a vision-based target geo-location technique that uses camera equipped unmanned air vehicles. They jointly estimate the target's position and the vehicles's attitude errors using linear regression resulting in improved target geo-localization. A salient feature of target geo-localization using bearing and range based sensors is the dependence of the measurement uncertainty on the position of the sensor relative to the target. Therefore, the influence of input parameters on nonlinear estimation problems, can be exploited to derive the optimal geometric configurations of a team of sensing platforms. However, maintenance of optimal configurations is not feasible given constraints on the kinematics of typical fixed wing aircraft. Frew [8] evaluated the sensitivity of the target geo-localization to orbit coordination, which enables the design of cooperative line of sight controllers that are robust to variations in the sensor measurement uncertainty and the dynamics of the target tracked. The existing geo-localization techniques are developed for stationary targets, in this paper, we detail a geo-localization technique for mobile ground targets using a camera mounted on a small fixed wing UAV.

Several researchers have used Multiple UAVs for cooperative geo-localization [10, 11, 12], because multi-agent platform provides several advantages including robustness, scalability, and access to more target localization information. The localization information computed at different UAVs can be fused to improve the target geo-location accuracy. The information fusion can be performed either in centralized or distributed manner. However, irrespective of the information fusion method, centralized or distributed, it is important to find out if geo-location estimates computed at two different UAVs belongs to the same target or to two different targets. The first approach is known as distance based approach where if the Mahalonobis distance [13] between two estimates is less then a threshold then the state estimates belong to same target otherwise to two different targets. Some of the distance based data association methods include the nearest neighbor(NN) method [14], probabilistic data association (PDA) [13], and joint probabilistic data association (JPDA) [15]. The second approach is known as appearance or view based data association, which is described in [16] and references therein. The existing data association techniques had been successfully demonstrated either for stationary targets or moving targets sensed either from stationary sensors or sensors mounted on ground robots or small UAVs used for indoor navigation (e.g., quad-rotors). However, the existing data association techniques cannot provide desired accuracy for small fixed wing UAVs. Small fixed wing UAVs imagery, attitude estimates, and UAVs position estimates from GPS are highly noisy which results in target geo-location estimates with high uncertainty. Therefore the distance based data association techniques will lead to high rate of false alarms and miss detection. On the contrary, appearance based data association methods are not affected by uncertainties in target location estimates. However, these methods are computationally expensive, and since small fixed UAVs have limited computation resources, they cannot be implemented onboard small UAVs . Furthermore, the low resolution imagery and altitude of UAVs result in small number target pixels in image, therefore, there are not enough features to perform view based data association.

In this paper, we discuss geo-localization of moving targets using pixel measurements from a camera onborad small fixed wing UAVs. Next, we formulate a hypothesis based on Bayes detection theory and develop a log likelihood ratio test to find if target location estimates from two different UAVs using EO sensor belongs to a same target or to two different targets. We show that the log likelihood ratio test has high probability of correct data association and low probability of false alarm under high errors in position and attitude of the UAVs. Also the test is computationally inexpensive, therefore, it can be used real time onboard on smaller fixed wing UAVs.

Rest of the paper is organized as follows. In Section 2, we detail the vison based geo-location of a moving target using a gimballed EO/IR camera on board a fixed-wing UAV. In Section 3, we develop a log likelihood ratio for determining the correspondence among the target state estimates. In Section 4, we present simulation results and probability of correct association and probability of false alarm. Finally, in Section 5, we give our conclusions.

2 Geo-location

In this section, we detail a technique of geo-localizing a mobile target in inertial coordinate using gimballed EO/IR camera on board a small fixed-wing UAV. We assume that the targets are detected with probability one. The technique presented here is an extension of geo-localization technique for a stationary target [17] to a mobile target.

In this paper, we use the camera model detailed in [17], which is shown in Figure 1, where f is the focal length in the unit of pixels and P converts pixels to meters. The location of the projection of the target is expressed in the camera frame as $(P\varepsilon_x,\ P\varepsilon_y,\ Pf)$, where ε_x and ε_y are the pixel location, in units of pixels, of the target. The distance from the origin of the camera frame to the pixel location $(\varepsilon_x,\ \varepsilon_y)$, as shown in Figure 1, is PF where

$$F = \sqrt{f^2 + \varepsilon_x^2 + \varepsilon_y^2}. \tag{1}$$

Finally using Figure 1, we can write expression for the unit direction vector as

$$\check{l}^c = \frac{l^c}{\mathbb{L}} = \frac{1}{\sqrt{\varepsilon_x^2 + \varepsilon_y^2 + f^2}} \begin{pmatrix} \varepsilon_x \\ \varepsilon_x \\ f \end{pmatrix}. \tag{2}$$

Let $l = p_t^i - p_{uav}^i$ be the relative position vector between the moving target and UAV, where $p_{uav}^i = (p_n, p_e, p_d)^\top$ is UAVs (north, east, down) position in inertial frame measured by an onboard GPS receiver and $p_t^i = (t_n, t_e, 0)^\top$ is target's (north, east, down) position in inertial frame. We define $\mathbb{L} = ||l||$ and $\check{l} = \frac{l}{\mathbb{L}}$. From geometry, we have relationship

$$
\begin{aligned}
p_t^i &= p_{uav}^i + \mathscr{R}_b^i \mathscr{R}_g^b \mathscr{R}_c^g l^c, \\
&= p_{uav}^i + \mathbb{L}(\mathscr{R}_b^i \mathscr{R}_g^b \mathscr{R}_c^g \check{l}^c),
\end{aligned} \tag{3}
$$

where $\mathscr{R}_b^i = \mathscr{R}_b^i(\phi, \theta, \psi)$ is rotation matrix from body to inertial frame, $\mathscr{R}_g^b = \mathscr{R}_g^b(\alpha_{az}, \alpha_{el})$ is the rotation matrix from gimbal to body frame, and $\mathscr{R}_c^g$ is the rotation matrix from camera to gimbal frame. We assume that UAV's attitude $(\phi,\ \theta, \psi)^\top$ (roll, pitch, yaw) is available for geo-localization. We also assume that the gimbal azimuth and elevation angles $(\alpha_{az}, \alpha_{el})$ are available and use the controller detailed in [17] to point the camera in the direction of the target.

The objective of geo-localization problem is to estimate range to target $\mathbb{L}$, which can be estimated using the flat earth model as shown in Figure 2. If UAV's height above ground $h = -p_d$ is known then the range estimate can be computed as

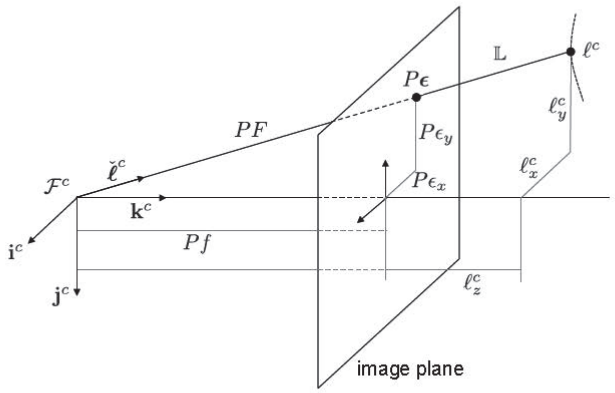

Fig. 1 [17] The camera frame. The target in the camera frame is represented by l^c. The projection of the target onto the image plane is represented by ε. The pixel location $(0,0)$ corresponds to the center of the image, which is assumed to be aligned with the optical axis. The distance to the target is given by $\mathbb{L}$. ε and f are in units of pixels. l is in units of meters.

$$\mathbb{L} = \frac{h}{\mathbf{k}^i \cdot \mathscr{R}_b^i \mathscr{R}_g^b \mathscr{R}_c^g \check{l}^c}, \tag{4}$$

where $\mathbf{k}^i$ is the unit vector in inertial frame pointing towards the center of the earth.

Using the flat earth model, we can write the expression for the geo-location estimate as

$$p_t^i = p_{uav}^i + h \frac{\mathscr{R}_b^i \mathscr{R}_g^b \mathscr{R}_c^g \check{l}^c}{\mathbf{k}^i \cdot \mathscr{R}_b^i \mathscr{R}_g^b \mathscr{R}_c^g \check{l}^c}. \tag{5}$$

2.1 Geo-location Using Extended Kalman Filter

The geo-location estimate in Equation (5) provides a one-shot estimate of the target location. Unfortunately, this equation is highly sensitive to measurement errors, especially attitude estimation errors of the airframe. Also, velocity and heading of the target also need to be estimated. In this section we will describe the use of the extended kalman filter (EKF) to estimate the location, velocity , and heading of a mobile ground target. Rearranging (5), we get

$$p_{uav}^i = h(x) = p_t^i - \mathbb{L} \mathscr{R}_b^i \mathscr{R}_g^b \mathscr{R}_c^g \check{l}^c \tag{6}$$

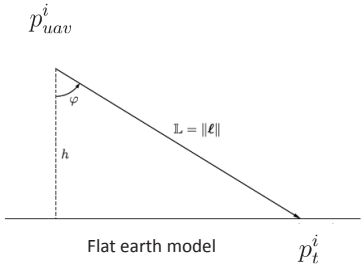

Fig. 2 Range estimation using flat-earth assumption.

which, since p^i_{uav} is measured by GPS, will be used as the measurement equation, assuming that GPS noise is zero-mean Gaussian.

We assume that the ground mobile target moves with constant velocity but can change its heading instantaneously. The target position $p^i_t = [t_n\ t_e\ 0]$ consist of north and east position coordinates and the target motion model can be written as

$$\dot{p}^i_t = \begin{pmatrix} v_n \\ v_e \\ 0 \end{pmatrix}, \tag{7}$$

where v_n is the velocity of UAV in north direction and v_e is the velocity of UAV in east direction.

Since $\mathbb{L} = ||p^i_t - p^i_{uav}||$, we have

$$\dot{\mathbb{L}} = \frac{(p^i_t - p^i_{uav})\top(\dot{p}^i_t - \dot{p}^i_{uav})}{\mathbb{L}}, \tag{8}$$

where for constant altitude flight, $\dot{p}^i_{uav}$ can be approximated as

$$\dot{p}^i_{uav} = \begin{pmatrix} \hat{V}_g \cos\hat{\chi} \\ \hat{V}_g \cos\hat{\chi} \\ 0 \end{pmatrix}, \tag{9}$$

and where $\hat{V}_g$ and $\hat{\chi}$ are estimated ground speed and course angle respectively using a EKF as discussed in [17]. The input to the geo-localization algorithm is the position and the ground speed of the MAV in the inertial frame as estimated by GPS described in [17], the estimate of the line-of-sight vector as given in (2), and the attitude as estimated by EKF described in [17].

The geo-localization algorithm is an EKF with state

$$\hat{x}_t = [\hat{t}_n, \hat{t}_e, \hat{\mathbb{L}}, \hat{v}_n, \hat{v}_e]^\top, \tag{10}$$

where $\hat{t}_n$ is the estimated target north position, $\hat{t}_e$ is the estimated target east position, $\hat{\mathbb{L}}$ is the estimated distance between target and the UAV, $\hat{v}_n$ is the estimated target velocity in north direction, and $\hat{v}_e$ is the estimated target velocity in east direction. The prediction equation can be written as

$$\dot{\hat{x}}_t = f(x) = \begin{pmatrix} \hat{v}_n \\ \hat{v}_e \\ \frac{(\hat{p}^i_t - \hat{p}^i_{uav})\top(\dot{\hat{p}}^i_t - \dot{\hat{p}}^i_{uav})}{\hat{\mathbb{L}}} \\ 0 \\ 0 \end{pmatrix}. \tag{11}$$

3 Target Discrimination using Bayes Detection Theory

In this section, we discuss the problem of target discrimination required for information fusion. Before information fusion it is important to find if the state estimates from two different platforms belongs to a same target or to two different targets. To solve this problem we use Bayes Detection theory [18] to develop a log likelihood ratio test.

Let us assume that, under hypothesis H_1, the estimates from two different UAV platforms are of same target, and under H_0 the estimates from two UAV platforms belong to two different targets.

Let $X_1 \in N[m_1(t), P_1(t)]$ and $X_2 \in N[m_2(t), P_2(t)]$ be the target state estimate of two UAVs (excluding range between an UAV and a target), where m and P are the mean and covariance respectively. We define a new random variable $Y = X_1 - X_2$, which is random variable with Gaussian pdf

$$Y \in N[m^y, P^y],$$

where $m^y = m_1 - m_2$ and $P^y = P_1 + P1$. If X_1 and X_2 are estimates of the same target then $m^y = 0$ other wise $m^y \neq 0$. We assume following two initial distribution

$$P[X_1 = X_2] = \tau,$$
$$P[X_1 \neq X_2] = 1 - \tau,$$

where $0 \leq \tau \leq 1$ is the probability of two targets being same. We sample the output each sampling period and obtain n samples. In other words

$$H_1 : Y_i \in N[0, P_i^y],$$
$$H_0 : Y_i \in N[m_i^y, P_i^y].$$

The probability density of Y_i under each hypothesis is

$$f_{(Y_i|X_1=X_2)} = \frac{1}{(2\pi)^{\frac{n}{2}}|P_i^y|^{\frac{1}{2}}} \exp\left[-\frac{1}{2}(y_i^\top (P_i^y)^{-1} y_i)\right],$$
$$f_{(Y_i|X_1\neq X_2)} = \frac{1}{(2\pi)^{\frac{n}{2}}|P_i^y|^{\frac{1}{2}}} \exp\left[-\frac{1}{2}(y_i - m_i^y)^\top (P_i^y)^{-1}(y_i - m_i^y)\right].$$

Because the Y_i are not independent, we cannot write the joint probability density of $Y_1, \cdots, Y_n$ simply as the product of the individual probability. However, we can write the joint probability using Bayes chain rule and conditional probability.

$$
\begin{aligned}
f_{(Y_1,\cdots,Y_n|X_1=X_2)} &= f_{(Y_n|Y_n-1)} f_{(Y_n-1|Y_n-2)} \cdots f_{(Y_2|Y_1)} f_{(Y_1)}, \\
&= \prod_{i=1}^{n} \frac{1}{(2\pi)^{\frac{n}{2}} |P_i^y|^{\frac{1}{2}}} \exp\left[-\frac{1}{2}(y_i^\top (P_i^y)^{-1} y_i)\right], \\
f_{(Y_1,\cdots,Y_n|X_1\neq X_2)} &= f_{(Y_n|Y_n-1)} f_{(Y_n-1|Y_n-2)} \cdots f_{(Y_2|Y_1)} f_{(Y_1)}, \\
&= \prod_{i=1}^{n} \frac{1}{(2\pi)^{\frac{n}{2}} |P_i^y|^{\frac{1}{2}}} \exp\left[-\frac{1}{2}(y_i - m_i^y)^\top (P_i^y)^{-1} (y_i - m_i^y)\right].
\end{aligned}
$$

The likelihood ratio can be written as

$$
\begin{aligned}
l(y_1,\cdots,y_n) &= \frac{f_{(Y_1,\cdots,Y_n|X_1=X_2)}}{f_{(Y_1,\cdots,Y_n|X_1\neq X_2)}}, \\
&= \frac{\prod_{i=1}^{n} \frac{1}{(2\pi)^{\frac{n}{2}} |P_i^y|^{\frac{1}{2}}} \exp\left[-\frac{1}{2}(y_i^\top (P_i^y)^{-1} y_i)\right]}{\prod_{i=1}^{n} \frac{1}{(2\pi)^{\frac{n}{2}} |P_i^y|^{\frac{1}{2}}} \exp\left[-\frac{1}{2}(y_i - m_i^y)^\top (P_i^y)^{-1} (y_i - m_i^y)\right]}.
\end{aligned}
$$

After canceling common terms and taking the logarithm, we have

$$
\log l(y_1,\cdots,y_n) = \frac{1}{2} \sum_{i=1}^{n} (m_i^y)^\top (P_i^y)^{-1} m_i^y - \sum_{i=1}^{n} (m_i^y)^\top (P_i^y)^{-1} y_i,
$$

from which likelihood ratio test can be written as

$$
\phi_\tau(y_1,\cdots,y_n) = \begin{cases} 1 \; if \; \log l(y_1,\cdots,y_n) > \log \frac{1-\tau}{\tau} \\ 0 \; if \qquad\qquad otherwise \end{cases} \tag{12}
$$

In other words, $\phi_\tau(y_1,\cdots,y_n) = 1$ means that target state estimates computed at different UAVs belong to the same target, and $\phi_\tau(y_1,\cdots,y_n) = 0$ means that the target state estimates belong to two different targets. We can compute probability of false alarm or incorrect data association as

$$
\begin{aligned}
P_{FA} &= P[\phi_\tau(y_1,\cdots,y_n) = 1 | Y_1 \neq Y_2], \\
&= E_{Y_1\neq Y_2} \phi_\tau(y_1,\cdots,y_n).
\end{aligned}
$$

Similarly, we can compute probability of correct data association

$$
\begin{aligned}
P_D &= P[\phi_\tau(y_1,\cdots,y_n) = 1 | Y_1 = Y_2], \\
&= E_{Y_1=Y_2} \phi_\tau(y_1,\cdots,y_n).
\end{aligned}
$$

Clearly, P_{FA} and P_D depends on assumed a priori distribution τ, number of samples, m^y, and P^y. Since, we are dealing with multi-dimensional normal pdfs, the integration in above expressions cannot be computed directly. However in the next section, we will compute P_{FA} and P_D using simulations.

4 Results

In this section, we develop a simulation environment in MATLAB/Simulink to geo-localize mobile targets using two fixed wing UAVs and analyze the log likelihood ratio test developed in the previous section. Figure 3 and Figure 4 show the simulation snap shots of two different scenarios we are considering in this paper. In Figure 3 two different UAVs are geo-localizing a same ground moving target, which is in field-of-view of both the UAVs. On the other hand, in Figure 4 two different UAVs are geo-localizing two different ground targets moving in same direction with same velocity. Objective is to use the log likelihood test (12) to determine if the target state estimates computed at two different UAVs are of a same target or two different targets.

First, we show results of geo-location of a target using a single UAV. Some of the important parameters used in the simulations are as follows

- GPS error variance: $[\sigma_n = 15m,\ \sigma_e = 15m,\ \sigma_d = 20m]$,
- UAV attitude error variance: $\sigma_{att} = 0.1\ rad$,
- Target speed $V_t = 5\ m/s$,

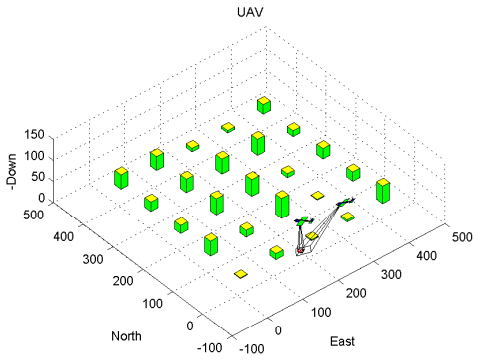

Fig. 3 UAV based geo-location: Two UAVs geo-localizing a single ground moving target.

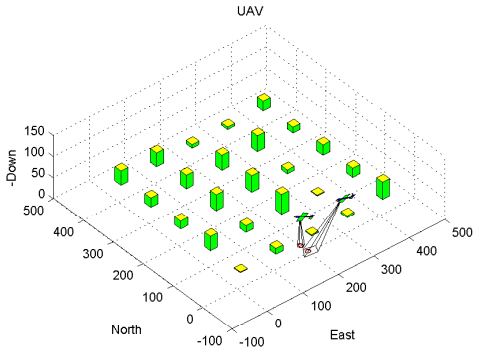

Fig. 4 UAV based geo-location: Two UAVs geo-localizing two different ground moving target.

- UAV air speed $V_a = 20\ m/s$.

Figure 5 shows the actual and estimated trajectory of a ground moving target. It can be seen that the estimated trajectory has the same behavior but has significant amount of uncertainty. The location estimates are very sensitive to the UAV attitude errors, more the errors in UAV attitude error more uncertainty in location estimates of the target. Figure 6 shows the actual and estimated velocities of the target in x and y direction. It can be seen that the velocity estimates are quite noisy but unbiased because there is no measurement of absolute velocity of the target and it is derivative of the target position estimates.

Next we compute the distribution of $Y = X_1 - X_2$ for $X_1 = X_2$ and $X_1 \neq X_2$ at attitude errors $\sigma_{att} = 0.1\ rad$ and $\sigma_{att} = 0.6\ rad$ as shown in Figure 7 and Figure 8 respectively. It can be seen that the distribution of $X_1 = X_2$ and $X_1 \neq X_2$ are overlapped and this overlapping increase with increase in UAV attitude errors. These distribution also shows the challenge in discriminating the two distributions using limited amount limited amount of samples. Figure 9 and Figure 10 show the probability of correct association and probability of false alarm with respect to the parameter m^y at different level of UAV attitude errors. In Figure 10, we keep distance between two UAVs equal to m^y to compute the P_{FA}. It can be seen, from Figure 9, that the test provides accuracy greater then 90% for $m^y \geq 35\ m$ with low probability of false alarm. In Figure 11, we keep $m^y = 35m$ constant and plot P_{FA} with respect to actual distance between two targets for different UAV attitude errors. It can be seen that,

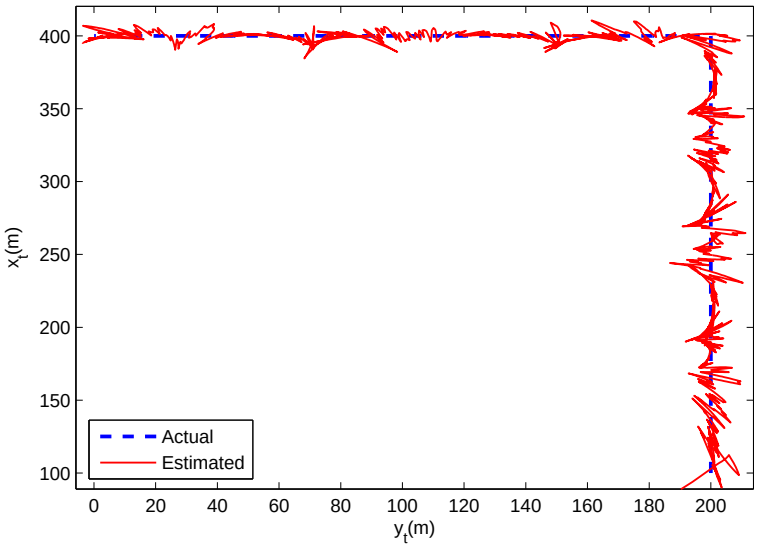

Fig. 5 UAV based geo-location: Actual and estimated trajectories of a ground moving target. The blue dashed curve and solid red curve represents the actual and estimated trajectories respectively.

even for this case, the P_{FA} is smaller then 0.01 after the distance between two targets is greater then $m^y = 35m$.

Simulation results presented in this section show that the Bayes log likelihood ratio test developed in this paper can discriminate targets which are very close and are moving in same direction with same velocity most of the time without requiring the appearance features. The test is computationally inexpensive and can be used realtime onboard UAVs to fuse information to accurately geo-localize ground moving targets.

5 Conclusions

In this paper, we have detailed a technique for geo-localization of moving targets using pixel measurements from a camera mounted on a fixed wing UAV. We have formulated a hypothesis based on Bayes detection theory and developed a log likelihood ratio to find if target state estimates computed at two different UAVs using EO sensor are of the same target or of two different targets. We have shown that the test for finding correspondence has high probability of correct data association and low probability of false alarm under high errors in UAV position and attitude errors.

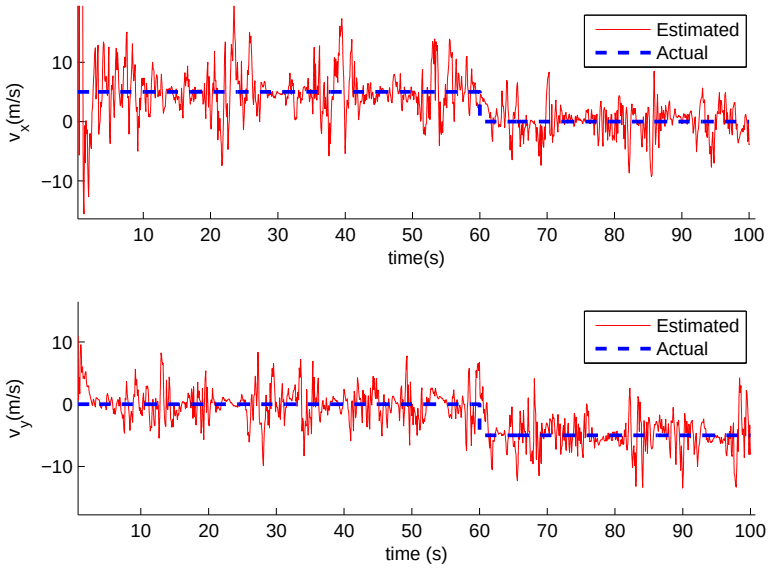

Fig. 6 UAV based geo-location:Velocity estimates of a ground moving target in x and y direction. The blue dashed curve and solid red curve represents the actual and estimated velocities respectively.

Also the Bayes log likelihood ratio test is computationally inexpensive, therefore, it can be used real time onboard on smaller UAVs.

Currently, we have only addressed data association problem using simple binary hypothesis. Our future work will be to extend this test to discriminate multiple moving targets Geo-localized my multiple UAVs. Furthermore, we will explore the option of path planning of UAVs to improve the probability of correct association while minimizing probability of false alarm. It is also important to find out how the altitude of the UAV effects the accuracy of the algorithm.

References

1. M. Quigley, M. A. Goodrich, S. Griffiths, A. Eldredge, and R. W. Beard, "Target acquisition, localization, and surveillance using a fixed-wing mini-UAV and gimbaled camera," in *Proc. IEEE Int. Conf. Robotics and Automation ICRA 2005*, 2005, pp. 2600–2605.
2. A. Ayyagari, J. P. Harrang, and S. Ray, "Airborne information and reconnaissance network," in *Proc. IEEE Military Communications Conf. MILCOM '96*, vol. 1, 1996, pp. 230–234.
3. R. W. Beard and T. W. McLain, "Multiple UAV cooperative search under collision avoidance and limited range communication constraints," in *Proc. 42nd IEEE Conference on Decision and Control*, vol. 1, 9–12 Dec. 2003, pp. 25–30.
4. D. W. Casbeer, R. W. Beard, T. W. McLain, S.-M. Li, and R. K. Mehra, "Forest fire monitoring with multiple small UAVs," in *Proc. American Control Conf the 2005*, 2005, pp. 3530–3535.
5. P. B. Sujit, D. Kingston, and R. Beard, "Cooperative forest fire monitoring using multiple UAVs," in *Proc. 46th IEEE Conf. Decision and Control*, 2007, pp. 4875–4880.

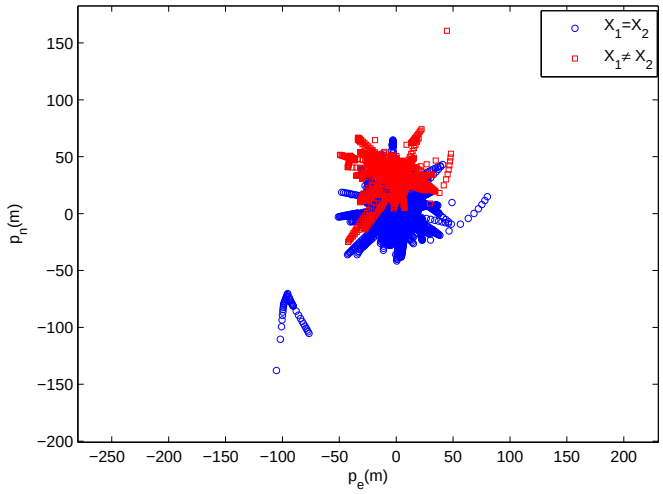

Fig. 7 This figure shows the distribution of random variable $Y = X_1 - X_2$ for $X_1 = X_2$ and $X_1 \neq X_2$ at attitude errors $\sigma_{att} = 0.1$ *rad* and $35m$ of distance between two targets. The blue circles represent distribution of $X_1 = X_2$ and red squares represent $X_1 \neq X_2$.

6. M. Pachter, N. Ceccarelli, and P. R. Chandler, "Vision-based target geo-location using camera equipped MAVs," in *Proc. 46th IEEE Conf. Decision and Control*, 2007, pp. 2333–2338.
7. D. B. Barber, J. D. Redding, T. W. McLain, R. W. Beard, and C. N. Taylor, "Vision-based target geo-location using a fixed-wing miniature air vehicle," *Journal of Intelligent and Robotic Systems*, vol. vol 47, no. 4, December, 2006.
8. E. W. Frew, "Sensitivity of cooperative target geolocalization to orbit coordination," *Journal of Guidance, Control, and Dynamics*, vol. vol 31, no. 4, August, 2008.
9. J. A. Ross, B. R. Geiger, G. L. Sinsley, J. F. Horn, L. N. Long, and A. F. Niessner, "Vision-based target geolocation and optimal surveillance on an unmanned aerial vehicle," in *AIAA, Guidance, Navigation, and Control Confrence, Honolulu, Hawaii*, Aug. 2008.
10. R. Olfati-Saber, "Distributed kalman filter with embedded consensus filters," in *Proc. and 2005 European Control Conference Decision and Control CDC-ECC '05. 44th IEEE Conference on*, Dec. 12–15, 2005, pp. 8179–8184.
11. W. Niehsen, "Information fusion based on fast covariance intersection filtering," in *Proc. Fifth International Conference on Information Fusion*, vol. 2, 8–11 July 2002, pp. 901–904.
12. D. W. Casbeer and R. Beard, "Distributed information filtering using consensus filters," in *Proc. ACC '09. American Control Conference*, Jun. 10–12, 2009, pp. 1882–1887.
13. T. Kirubarajan and B.-S. Yakov, "Probabilistic Data Association Techniques for Target Tracking in Clutter," *Proceedings of the IEEE*, vol. 92, no. 3, pp. 536–537, 2004.
14. J. J. Leonard, H. F. Durrant-Whyte, and I. J. Cox, "Dynamic map building for an autonomous mobile robot," *The International Journal of Robotics Research*, vol. 11, no. 4, pp. 286–298, 1992. [Online]. Available: http://ijr.sagepub.com/content/11/4/286.abstract
15. B.-S. Yaakov and E. F. Thomas, *Tracking and Data Association*. Academic, NewYork, 1988.
16. A. Gil, O. Reinoso, O. Mozos, C. Stachnissi, and W. Burgard, "Improving data association in vision-based SLAM," in *2006 IEEE/RSJ International Conference on Intelligent Robots and Systems,*, 2006.
17. R. Beard and T. W. McLain, *Small Unmanned Aircraft: Theory and practice*. Princeton university press, 2011.

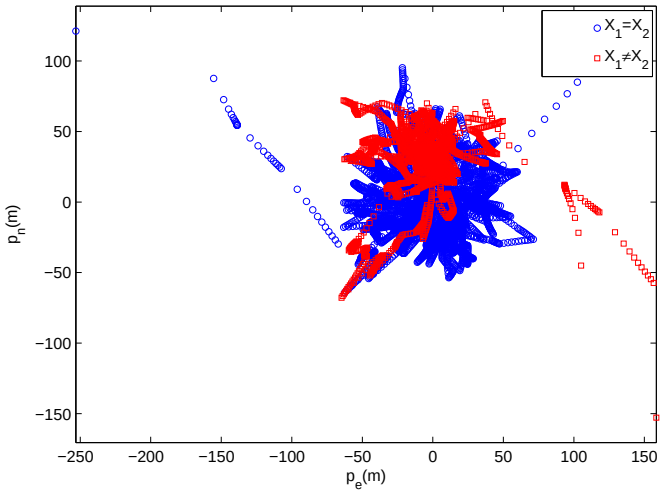

Fig. 8 This figure shows the distribution of random variable $Y = X_1 - X_2$ for $X_1 = X_2$ and $X_1 \neq X_2$ at attitude errors $\sigma_{att} = 0.6$ *rad* and $35m$ of distance between two targets. The blue circles represent distribution of $X_1 = X_2$ and red squares represent $X_1 \neq X_2$.

18. T. K. Moon and W. C. Stirling, *Mathematical Methods and Algorithms in Signal Processing*. Prentice-Hall, Upper Saddle River, NJ, 2000.

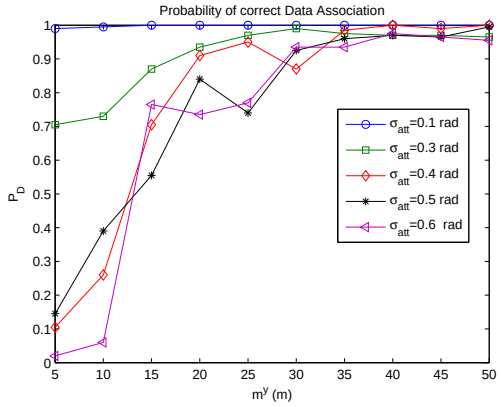

Fig. 9 This figure shows the probability of correct data association obtained using the likelihood test for different attitude errors and m^y. Each probability number is generated over 200 runs over $n = 20$ sample for each run.

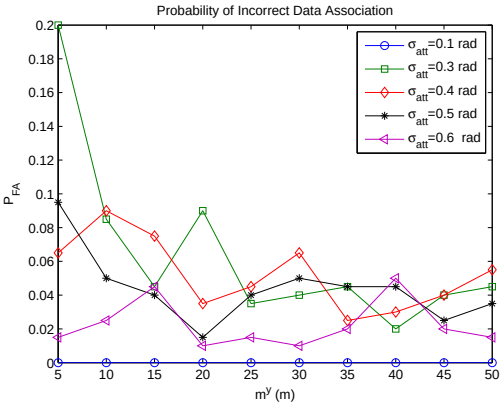

Fig. 10 This figure shows the probability of false alarm obtained using the likelihood ratio test for different attitude errors and m^y. Each probability number is generated over 200 runs over $n = 20$ sample for each run. Also for to generate these probabilities we assume that actual distance between two targets is equal to m^y.

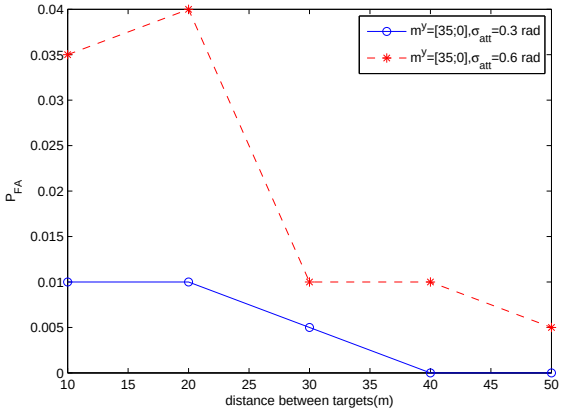

Fig. 11 This figure shows the probability of false alarm obtained using the likelihood ratio test for different attitude errors and distance between targets at a constant $m^y = [35;0]$.